Risley prisms applications: an overview

Guillermo Garcia-Torales

Electronic Department, CUCEI, University of Guadalajara, Av. Revolución 1500, Guadalajara, Jal. Mexico.

ABSTRACT

Risley prisms systems consist of two-wedge aligned prisms that deviate a light beam or wavefront. The relative angle between prisms determines the displacement of the central point wavefront. In the case of wavefront propagation through the Risley system, the relative angle also can introduce a controlled tilt. Then, the beam's or wavefront displacement direction is controlled by changing the relative angle between prisms. Risley prisms have been used in multiple applications such as super-resolution imaging and field of view (FOV) extension, steering systems, precision pointers, scanning systems, and wavefront alignment and positioning. This paper presents a description of the techniques used by Risley prisms making a compilation of their most essential characteristics. One of the related applications is reviewed on a Vectorial Shearing Interferometer. The paper overviews the advantages and disadvantages of using Risley prisms in different valuable applications.

Keywords: Risley prisms, shearing interferometry, pointing systems; scanning systems; wavefront alignment

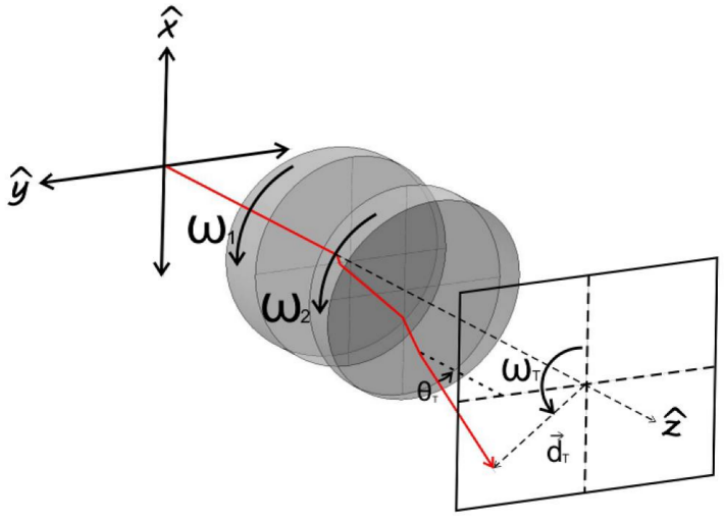

Figure 1. One ray is refracted at each surface through the Risley prism system. The prism orientations determine the amount of ray deviation. The angular orientation of both prisms (ω_1 and ω_2) determines the final ray deviation d_T in the observation plane.

1. INTRODUCTION

Risley prisms are two consecutive wedge prisms aligned, also named in a tandem configuration. Each prism has one surface normal to the optical axis, and each prism may rotate around the optical axis, deflecting the incident beam individually.[1] The optical axis is defined as the line of symmetry of other optical components in the system. The total deviation of the output beam d_T is controlled by the angular position of each prism and their separation, as is shown in Fig. 1.

Further author information: (Send correspondence to Guillermo Garcia-Torales)
G.G.T.: E-mail: garcia.torales@academicos.udg.mx

Advances in 3OM: Opto-Mechatronics, Opto-Mechanics, and Optical Metrology, edited by Virgil-Florin Duma, Jannick P. Rolland, Adrian G. H. Podoleanu, Proc. of SPIE Vol. 12170, 121700H
 · 0277-786X · doi: 10.1117/12.2616071

Figure 2 depicts one possible experimental configuration set up to characterize the performance of a Risley prism system. Both prisms are in air, the refraction index of the prisms n_p are equal and the apex angle α is the same in both prisms. A He–Ne laser beam is deviated by the prism system. The beam is incident on the observation plane with a deviation d_T. The beam spot in the observation plane is captured by a CMOS camera. L is the distance from the prism system to the observation plane measured along the optical axis. S is the inter-prism distance. L_C is the distance between the camera and the observation plane. W_1 and W_2 are the central thickness along the optical axis of the first and the second prism, respectively.

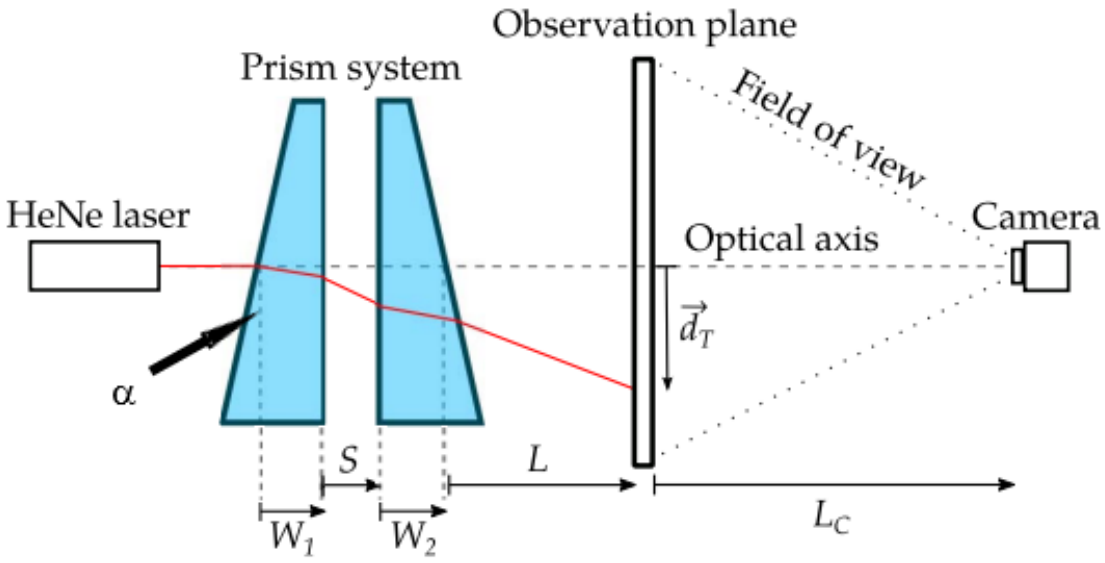

Figure 2. Diagram of a typical experimental setup using a laser as radiation source and a camera for the acquisition image.

This paper assumes the paraxial approximation method of modeling each prism as a thin prism. In the paraxial approximation, the deviation produced by a single prism is independent of the position of the surface normal to the optical axis. The deviation angle θ_T considering the individual angles of rotation of two identical prisms (ω_1 and ω_2) is calculated by:

$$\theta_T = \left[2(n_p - 1)\,\alpha\, cos\left(\frac{\omega_1 - \omega_2}{2}\right)\right]. \tag{1}$$

The displacement d_T, produced by the action of two rotated prisms, is proportional to the distance of the detection plane from the last surface of the second prism L.

$$d_T = L\, tan\ \left[2(n_p - 1)\,\alpha\, cos\left(\frac{\omega_1 - \omega_2}{2}\right)\right]. \tag{2}$$

There are four possible Risley prism configurations with a pair of wedge prisms shown in Fig.3. In most Risley prisms configurations, one prism plane face is usually oriented with its normal parallel to the optical axis. To the apex angle, the side that is normal to the optical axis contains the aperture traditionally named by the diameter; the hypotenuse has held the face with the slope defined by the apex angle, and the side opposite is the base of the prism. The four configurations present similar beam deviation through the prism system. Fig. 3(a) and 3(b) are the most used. Figure 3(a) is selected in many steering and scanning systems. In contrast, Fig 3(b) is considered preferable when the distance between prisms, S in Fig. 2, is used as a parameter to control the phase of a wavefront, e.i., phase shifters systems.

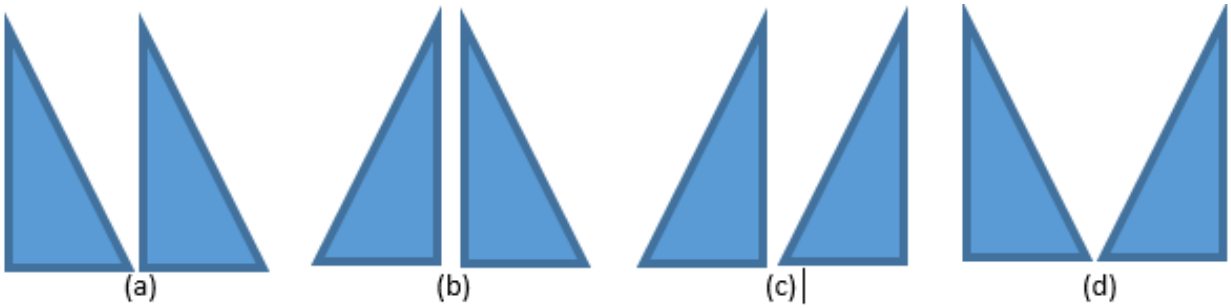

Figure 3. Four possible configuration for the Risley prism system. Figures 3(a) and 3(b) are the prisms configurations most commonly used in steering scanning and phase shifting applications.

Drawbacks in Risley prisms are well identified.[2] One of the most common problems is the blind spot around the optical axis. The blind spot problem deals with the difficulties of steering beams in the proximity of the optical axis. In the most used two-prisms configuration, the alignment of the prisms, the finite size of the prisms, and its mounting systems precise the space between the prisms. This space between prisms, the inter-prism distance, introduces a constant deviation from the optical axis even with two Risley prisms accurately matched, avoiding steering the beam along the optical axis. Resulting from the blind spot problem appears the singularity problem. This case requires an excessive prism rotation speed to generate large prisms rotation to move toward the optical axis.

Another problem is the nonlinearity that introduces distortion. The angular variation depends on the rotations that trace displacement with a solenoidal dependence. Control equations can solve nonlinearities for local linearization. However, physical restriction of shape and materials appears always. Finally, the mechanical tolerances, the accuracy in the wedge angle, the errors in alignment, temperature, and pressure variations affect the system's degree of sensitivity, accuracy, precision, and resolution.

2. RISLEY PRISMS DEVIATE RAYS AND WAVEFRONTS

In numerous applications, a laser beam deviated by a Risley prisms syst is narrow and may be considered a ray propagated along with the system. Often, the deviation of a laser ray propagated from a point source to the plane of observation is detected without being concerned about the beam spot's diameter but the position in a time instant. In some cases, the spot's phase is less important than its position, and then the phase is not considered.[3,4]

Otherwise, when the beam diameter is relevant.[5] The beam spot is not considered a point but a plane collimated wavefront. After the wavefront pass through the system, it also deviates its direction as formerly was explained, but at the same time, the position relative of prisms introduces a wavefront tilt. This tilt introduces a linear phase change at any direction around the ray at the wavefront center proportional to the deviation angle between prisms. Significant deviation angles may generate large wavefront tilt. The rotation angles and the separation between prisms change the phase allowed by the prism's thickness material.

Many other remarkable and interesting applications not in the above categories are also published.[6–8] In these cases, the authors report Risley prisms as neutral density filters,[9] a confocal interferometer,[10] and forward and inverse solutions for applications with three elements Risley prisms.[11] We may remember that the first prism application includes the ophthalmoscopic proposal out of the scope of this paper.[12] Ophthalmologists initially used Risley prisms to measure binocular accommodation and thus had a relatively small angular range. More recently, Risley prisms have been designed to cover a wide range of angles and have been achromatized to minimize chromatic variations in steering direction.[13,14] Risley prism scan-based approach to standoff trace explosive detection.[15]

2.1 Risley prisms used in steering and scanning systems

Risley prisms are widely used in many applications considering a beam emitted from a laser source.[16] Firstly, when the rotation of each prism is continuous and in a defined direction. In this case, the differences in velocity and direction of rotation of the prisms are considered program-specific prisms rotation routines. This methodology is used in the case of beam steering/tracking[17–21] and laser scanning applications.[22–27]

The second approach considers a point in discrete but variable, rotation of a narrow beam to pointing a specific coordinate in a space defined by a plane or expanding the field of view, FOV.[28] It is helpful for image acquisition of cameras and signal detection in antennas or simply marking coordinates or objects within a specific environment. In the case of pointing applications, Risley prism performs angular displacement that becomes to a particular coordinate in a plane of interest. For beam direction, the Risley prisms present advantages compared to other beam steering systems due to their compactness and low sensitivity to vibration, robustness (relative insensitivity to vibration), independent rotational axes, low moment of inertia speed.

As already mentioned, the relationship between the final beam pointing position and the angular orientation of the prisms is not linear. This relationship involves two problems that we call the forward and the inverse problems.[29,30] The forward problem predicts the point where the beam is incident on the observation plane (finding the vector d_T) for a given angular orientation of the prisms, 1 and 2. In practice, the model for a wedge prism using the paraxial approximation is the thin prism equation. Using this equation, the deviation of the ray generated by a single prism may be calculated. The deviation caused by the two prisms is determined as the vector sum of the deviations generated by each prism individually. This approach is relatively easy to apply, and it is sufficiently precise for many applications. Unfortunately, this approximation underestimates the beam deviation that the prism generates and the effect of their separation on the ray direction.

Meanwhile, the exact ray tracing method provides the precise deviation of the beam for each angular orientation of the prisms. The inverse problem involves determining the angular direction of the prisms for the given coordinates of incidence in the observation plane. The forward and inverse problems have been extensively analyzed in the literature leading to the generally accepted conclusion that the exact solution is impossible.

Beam steering devices can point and track a laser beam within a field-of-regard (FOR), depending on the fill factor. The steering trajectories can be selected as discrete positions or random trajectories considering tiny angular prisms positioning the spot in a specific place for a required time on the detection plane. In contrast, scanning devices move the beam axis continuously, and switching devices can only ad address predefined directions. Reviews of current technologies for steering, scanning, and switching laser beams are found in references.[31–35]

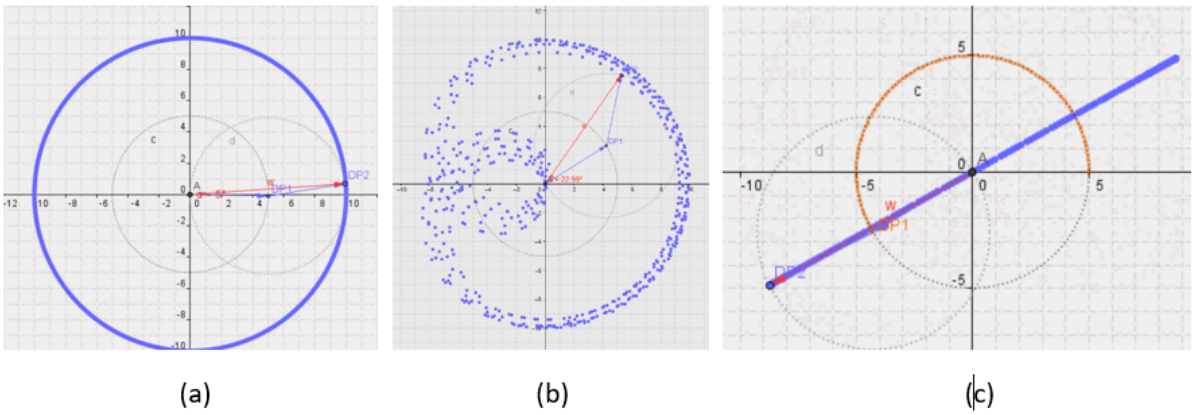

Figure 4. The steering system provides random and discrete displacements over the field of regard. (a) The larger displacement of each prism determines the FOR. (b) The plot of random points within the FOR defined positioning and marked specific coordinates. (c) A sequence of points that follow linear tracking.

Figure 4 shows simulations of the projected points at the detection plane generated by a steering system. Figure 4(a) shows the field of regard (FOR) for the Risley system configuration. The FOR is the functional area

where a point can be placed. The total deviation of the beam is the vector in red color, resultant of the sum of the individual deviation of each prism, DP 1 and DP 2, vectors in blue color.

Steering based in the Risley prism system allows both pointing and tracking possibilities. Fig. 4(b) shows many points plotted randomly. Some points are located at the edge of the FOR, others around the center of the FOR. The final position of each beam spot can be selected, and this is the case of a pointing system. A straight line is plotted in Fig. 4(c) using small and discrete increments routines. This trajectory may be used in tracking systems for objects with linear displacement over the FOR.

Scanning systems devices with Risley prisms are extensively used because of their compactness and high velocity. Exact scan patterns can be achieved with high-resolution systems. The scanning system with Risley prism present three basic scanning ways, linear, spiral, and described loops or petals, as is shown in Fig. 5. Figure 5(a) shows a sequence of lines traversing across a surface of the detection plane. In this case, the scanning only is plotted covering two sections in the plane, the first and third quadrant. The generated pattern by the back and forth of the spot describes a sequence of lines. This scanning sequence eventually encompasses all the FOR, Fig. 5(a). Another way to cover sequentially the FOR is by a kind of radial scanning. Figure 5(b) shows the spiral trace generated by the Risley prisms system that allows scanning from the center to the edge of the FOR. The scanning can also describe loops or petals, shown in figures 5 (c) and (d), or others described in detail in the literature. All the different Risley scanning patterns depend on the ratio of the rotation speeds, the balance of the beam deviations, and the relative orientation — namely, the phase angle of the prisms.

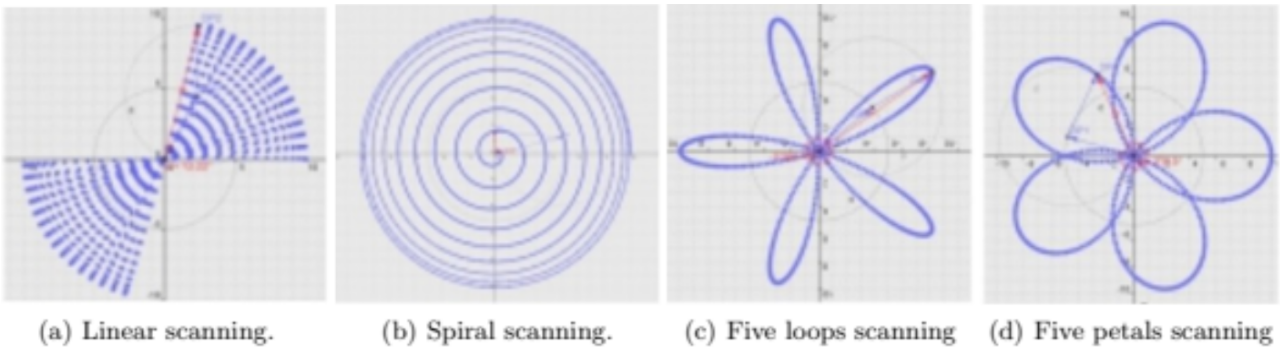

(a) Linear scanning. (b) Spiral scanning. (c) Five loops scanning (d) Five petals scanning

Figure 5. The scanning system with Risley prism present three basic scanning ways, linear, spiral (radial), and describing loops or petals.Fig.5(a) shows a sequence of lines traversing across a surface of the detection plane. This scanning sequence eventually encompasses all the FOR. Fig. 5(b) shows the spiral trace generated by the Risley prisms system that allows scanning from the center to the edge of the FOR. The characteristic Risley prisms scanning describes loops or petals. Fig. 5(c) shows five stretch loops and Fig. 5(d) has five wider loops.

2.2 Risley prisms used as a phase shifter

Next, we introduce the concept of wavefront formally, beyond its intuitive meaning. We recall that the radiation is an electromagnetic wave, characterized by its electric field vector and phase. Then the wave front of this wave is the surface in 3-D space that connects the points that have the same phase. When the radiation is emitted from a point source, such as a star, its wave front is spherical in the vicinity of the star, and planar at a far distant e.g. the Star-Earth distance.

The control of the position of a wavefront through the Risley system is being considered in some interferometric applications.[36] In this case, achromatization is a disadvantage of Risley prisms to their inherent chromatic aberration. It becomes an issue when the beam is not from a laser source, and it has a diameter that defines a wavefront. However, Risley prisms can be corrected for chromatic aberration combining materials having different refraction indices.[37]

In an interferometric system, the tilt on the wavefront introduces a controlled carrier in a selected direction.[38] In a shearing interferometer, it corresponds to the directional derivative in the case of infinitesimal angle variations

or shearing wavefront for incremental displacements. In both, cases, tilt introduces a linear phase change. The change in the tilt is proportional to the magnitude of the slope, the direction of the slope defines the orientation of the phase changes. These phase changes may be high precision ones, as small that can interact or compensate plane wavefronts, even if the slopes are so small, e.g., those that are coming from an extra-solar punctual source.[39–41]

Figure 6 shows a conceptual diagram showing the geometry for detecting a wavefront of a faint source, e.g., an extra-solar planet close to a bright star, using a Vectoral Shearing Interferometer, VSI. A planet out of the solar system emits a wavefront that is considered plane at the entrance pupil of the VSI. The VSI is a modified, by the Risley system, Mach-Zehnder interferometer. The prisms rotation in one arm of the VSI changes the tilt of the plane wavefront. After interference, an intensity patter of straight fringes may be generated. The number and orientation of the fringes provide information about the position and the orientation of the planet with respect to the optical axis of the VSI.

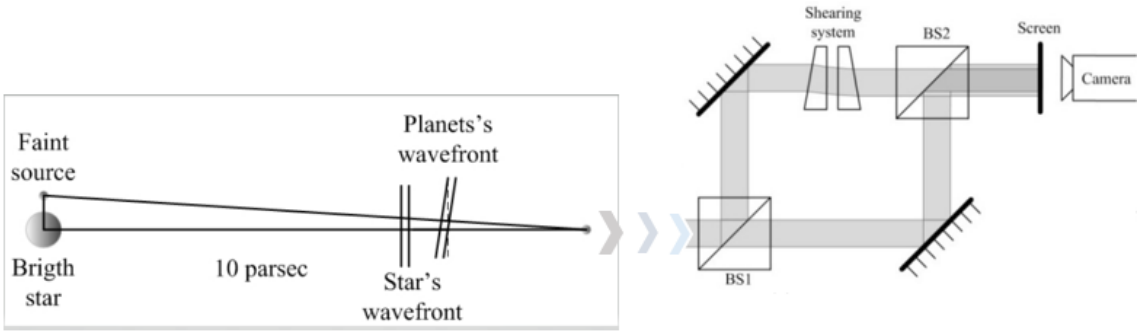

Figure 6. Risley prism application as a phase shifter. A planet out of the solar system emits a wavefront that is considered a plane at the entrance pupil of the VSI. VSI is a modified Mach-Zehnder interferometer. Geometry for the detection of a planet outside our solar system.

The shearing system of this interferometer determines the optical path difference of the sheared wavefront by wedge rotation, and then it may be considered a phase shifter. Compared with other mechanical shearing methods, the proposed instrument allows for higher displacement settings and varied orientations. It also offers the possibility of adapting to the present-d interests of automation. This instrument can generate fringe patterns that represent the directional derivative of the wavefront under analysis, practically in any spatial direction and trajectory. The difference in the optical path introduced by the Risley prism is used as a phase shifter that generates an intensity pattern. The intensity pattern approximated to a derivative by Taylor series expression is given in equation 3. The resulting interference pattern is composed of high-frequency fringes generated by the tilt and modulated by the wavefront derivative.

$$I(x,y) = \ I_0(x,y) + I_C(x,y) * cos^2\left(\frac{\partial W(x,y)}{\partial x}\Delta x + \frac{\partial W(x,y)}{\partial y}\Delta y + T(x,y)\right) \tag{3}$$

The simulated phase introduced by the Risley prism shown in figure 7. Fig. 7(a) shows the phase map in the FOR, when the angle relative between prisms is about one degree. The relative angle change the tilt orientation modifying the phase to the right in Fig. 7(b), and to the left in FIg. 7(c). The phase changes may occur when the wavefront from the extra-solar planet follows its natural orbit around the star. The rotation of the prisms could be aligned to compensate for the new direction of the tilt with respect to the VSI.

The phase maps represent the changes introduced by the slope resultant of the wavefront passing through the branch in the interferometer where the prism system acts as a phase shifter when the prism system is placed in one arm of the VSI as in Fig. 6, an intensity pattern is generated. The phase introduced in these simulations introduces phase changes in the order of a half wavelength. In this case, the apex $\alpha = 2°$, the relative angle of rotation $\omega_1 = 2°$ and $\omega_1 = 2°$ is about one degree. The total normalized deviations of θ_T oscillates between 0.994 to 1.

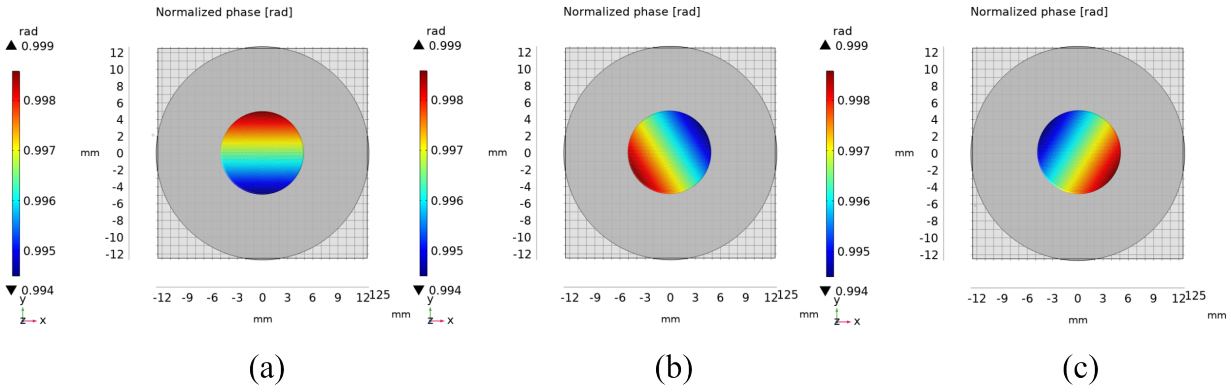

Figure 7. One possible phase map introduced by the Risley prisms tilt in a plane wavefront coming from a far source. The map corresponds to half wavefront tilt. The phase changes are linearly introduced and perpendicular to the tilt. Fig. 7(a) represents the aligned system. Figs. 7(b) and 7(c) represent changes of the position of the prisms according with the movement of the extra-solar planet.

However, the long-distance of the extra-solar planet to the interferometer should not generate a fringe pattern at all. The tilt magnitude just generates small variations in the intensity pattern. Figure 8 (a) to (c) shows the corresponding intensity patterns to the map phase in figure 7 (a) to (c). The small optical path difference results in an intensity pattern without fringes but smooth variations of intensity pattern. This result is according to the small phase changes that may be detected in the case of the planet's extra-solar detection. This possibility may occur when the tilt waterfronts are very small because of the long distance between the source and the detector. This problem should be solved with the interaction of several synchronized VSIs placed at a proper distance between them.

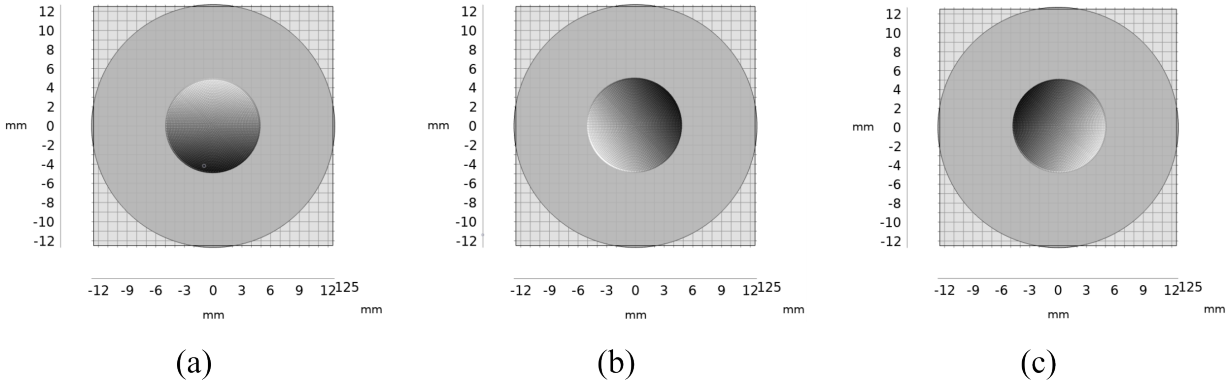

Figure 8. Intensity patterns generated in the VSI after interference considering rotations of the prisms as in Fig. 7 (a) to (c) respectively.

Considering the VSI is detecting a tilted wavefront, where the distance from the star-planet to Earth is big enough to consider the wavefront as a plane, a minimal pat of the spherical wavefront, the pattern observed will be an homogeneous intensity pattern on any direction we could rotate the shearing system. Figure 9 present the simulations of the intensity patterns of plane wavefronts from a planet far away from the detection system. The first row shows an uniform white pattern that means that the system is always compensating tilt, e.g. there is no path difference neither any tilt is introduced. The second and third rows shows three different patterns. The white one, corresponds to the rotations of the prisms that cancels tilt. The black one generated when there is not detection on that direction. Tilt in the x direction is compensating when the y direction is not sensible to this tilt, the tilt is parallel to the slope of the prisms. Tha last case, corresponds to those that their are components of tilt in both x and y directions. Her the intensity pattern looks like a gray level depending of the tilt of the

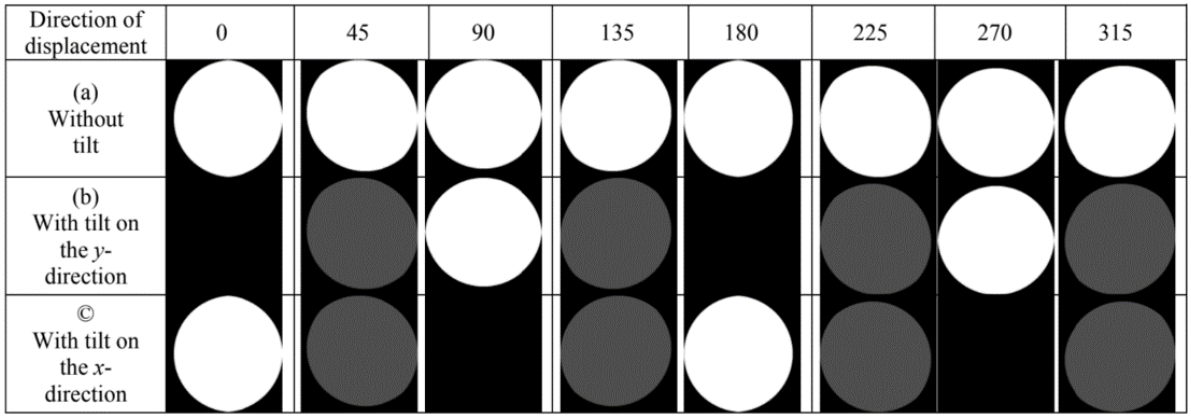

Figure 9. Intensity pattern generated in the VSI after interference considering different prisms rotations when the extra-solar planet is moving around the star. The first row shows the perfect alignment with the extra-solar planet tilt. Second and third rows show possible intensity patterns situations.

incident wavefront over the VSI.

Finally, Table 1 shows some critical parameters to consider in pointing, steering, scanning, and phase shifter applications when using Risley prisms. All the applications share similar restrictions and tolerances. Some apparent parameters define the application. The pointing accuracy and pointing thickness resolution are critical parameters in pointing and systems. The maximum and the steering angle control are essential in steering systems. In scanning systems, the ratio of rotation angles and the ratio of the rotational speed defined are relevant. Phase shifter requires high precision manufacturing tolerances and highly high alignment.

Table 1. Critical parameters to consider when the Risley prisms are used in pointing, steering, scanning and phase shifting applications.

POINTING	STEERING	SCANNING	PHASE SHIFTING
Field Of Regard (FOR)	Maximum steering angle	Speed	Clear aperture
Wavelength	Beam divergence	Resolution	Stiff tolerances
Wedge angle	Aperture	Precision	Precise alignment
Thickness pointing resolution	Spectral range	Compact and light	Extremely small apex angle
Dispersion	Cost	High precision rotation angles	Vibration
Pointing Accuracy	Throughput	Inertia	Fine mechanics
Slew rate	Control of the steering angle	Angular divergence	Resolution in arcsec
Control bandwidth	Vignetting	Ratio of the angles of the prisms;	Distortion compensation
Throughput	Imaging capability	Ratio of the rotational speeds	Achromatic correction
Wavefront quality	Alignment	Apertures of the prisms	Homogeneous materials
Operational temperature	Hysteresis	Rotational speeds	Small distance between Prisms

3. CONCLUSIONS

This work presents an overview of the applications of Risley prisms, considering two points of view. First, Risley prisms are used for displacements of a point or a narrow beam, either in discrete or continuous steps. Here, forward and inverse solutions solve the most practical pointing, steering, and scanning applications. A second approach is when the beam is considered as a wavefront. Here, the beam area and the phase changes introduced

by the Risley system have to be considered. In this case, Risley prisms are used as a phase shifter device. This phase shifter control results are helpful in shearing interferometry like in the Vectorial Shearing Interferometer, VSI. The variable sensitivity of the interferometer facilitates the detection and identification of tilted wavefronts, even with very small slopes. In this case, the rotation of the prisms wedges detects controls the orientation and amount of tilt represented by intensity patterns without fringe patterns. Still, gradients of intensity proportional to the wavefront were detected.

ACKNOWLEDGMENTS

The author acknowledges the Exact Science and Engineering University Center, CUCEI, for its acronym in Spanish, of the University of Guadalajara, Jalisco, Mexico, to accomplish this research. The author thanks to JRGR for the FEM graphics presented in this paper.

REFERENCES

[1] Sullivan, M. T., "Synopsis of 'risley prism beam pointer'," *Bearing a date of* , 1–5 (2006).

[2] Schwarze, C. et al., "A new look at risley prisms," *Photonics Spectra* **40**(6), 67–71 (2006).

[3] Ostaszewski, M., Harford, S., Doughty, N., Hoffman, C., Sanchez, M., Gutow, D., and Pierce, R., "Risley prism beam pointer," in [*Free-Space laser communications VI*], **6304**, 630406, International Society for Optics and Photonics (2006).

[4] Harford, S. T., Gutierrez, H., Newman, M., Pierce, R., Quakenbush, T., Wallace, J., and Bornstein, M., "Infrared risley beam pointer," in [*Free-Space Laser Communication and Atmospheric Propagation XXVI*], **8971**, 89710P, International Society for Optics and Photonics (2014).

[5] Bravo-Medina, B., Garcia-Torales, G., Legarda-Sáenz, R., and Flores, J. L., "Wavefront recovery fourier-based algorithm used in a vectorial shearing interferometer," in [*Infrared Remote Sensing and Instrumentation XXI*], **8867**, 88670Z, International Society for Optics and Photonics (2013).

[6] Sánchez, M. and Gutow, D., "Control laws for a three-element risley prism optical beam pointer," in [*Free-Space Laser Communications VI*], **6304**, 630403, International Society for Optics and Photonics (2006).

[7] Lu, S., Gao, M., Yang, Y., Zhu, R., Hou, X., Sun, J., Chen, W., and Zhu, X., "Inter-satellite laser communication system based on double risley prisms beam steering," *Applied optics* **58**(27), 7517–7522 (2019).

[8] Patel, S., Rajadhyaksha, M., Kirov, S., Li, Y., and Toledo-Crow, R., "Endoscopic laser scalpel for head and neck cancer surgery," in [*Photonic Therapeutics and Diagnostics VIII*], **8207**, 82071S, International Society for Optics and Photonics (2012).

[9] Duma, V.-F. and Nicolov, M., "Neutral density filters with risley prisms: analysis and design," *Applied optics* **48**(14), 2678–2685 (2009).

[10] Warger II, W. C., Guerrera, S. A., and DiMarzio, C. A., "Toward a compact dual-wedge point-scanning confocal reflectance microscope," in [*Three-Dimensional and Multidimensional Microscopy: Image Acquisition and Processing XIV*], **6443**, 644311, International Society for Optics and Photonics (2007).

[11] Li, A., Liu, X., and Sun, W., "Forward and inverse solutions for three-element risley prism beam scanners," *Optics express* **25**(7), 7677–7688 (2017).

[12] Risley, S. D., "A new rotary prism," *Transactions of the American Ophthalmological Society* **5**, 412 (1889).

[13] Lacoursiere, J., Doucet, M., Curatu, E. O., Savard, M., Verreault, S., Thibault, S., Chevrette, P. C., and Ricard, B., "Large-deviation achromatic risley prisms pointing systems," in [*Optical Scanning 2002*], **4773**, 123–131, International Society for Optics and Photonics (2002).

[14] Bos, P. J., Garcia, H., and Sergan, V., "Wide-angle achromatic prism beam steering for infrared countermeasures and imaging applications: solving the singularity problem in the two-prism design," *Optical Engineering* **46**(11), 113001 (2007).

[15] Schwarze, C. R., Schundler, E. C., Vaillancourt, R., Newbry, S. P., and Benedict-Gill, R., "Risley prism scan-based approach to standoff trace explosive detection," *Optical Engineering* **53**(2), 021110 (2013).

[16] Bravo-Medina, B., Strojnik, M., Garcia-Torales, G., Torres-Ortega, H., Estrada-Marmolejo, R., Beltrán-González, A., and Flores, J. L., "Error compensation in a pointing system based on risley prisms," *Applied optics* **56**(8), 2209–2216 (2017).

[17] Li, Y., "Third-order theory of the risley-prism-based beam steering system," *Applied optics* **50**(5), 679–686 (2011).

[18] Zhang, H., Yuan, Y., Su, L., and Huang, F., "Beam steering uncertainty analysis for risley prisms based on monte carlo simulation," *Optical Engineering* **56**(1), 014105 (2017).

[19] Li, A. and Liu, X., "Passive target tracking method based on vision information feedback," in [*Optical Modeling and Performance Predictions X*], **10743**, 107430Y, International Society for Optics and Photonics (2018).

[20] Zhou, Y., Chen, Y., Sun, L., Hu, F., Wang, Z., and Fan, S., "Analysis on key issues of boresight adjustment in imaging tracking based on risley prisms," *Optical Engineering* **59**(12), 123104 (2020).

[21] Lu, Y., Zhou, Y., Hei, M., and Fan, D., "Theoretical and experimental determination of steering mechanism for risley prism systems," *Applied optics* **52**(7), 1389–1398 (2013).

[22] Jeon, Y.-G., "Generalization of the first-order formula for analysis of scan patterns of risley prisms," *Optical Engineering* **50**(11), 113002 (2011).

[23] Lyu, J., Chen, Z., Wang, G., Tan, M., Lu, R., Cao, Z., and Liu, Y., "Extended risley scanning system with 30× 360 coverage," *Applied Optics* **60**(26), 8082–8087 (2021).

[24] Marshall, G. F., "Risley prism scan patterns," in [*Optical Scanning: Design and Application*], **3787**, 74–86, International Society for Optics and Photonics (1999).

[25] Duma, V.-F., "Laser scanners: from industrial to biomedical applications," in [*8th Iberoamerican Optics Meeting and 11th Latin American Meeting on Optics, Lasers, and Applications*], **8785**, 8785CU, International Society for Optics and Photonics (2013).

[26] Duma, V.-F., Rolland, J. P., and Podoleanu, A. G., "Perspectives of optical scanning in oct," in [*Design and Quality for Biomedical Technologies III*], **7556**, 75560B, International Society for Optics and Photonics (2010).

[27] García-Torales, G., Flores, J., and Muñoz, R. X., "High precision prism scanning system," in [*Sixth symposium optics in industry*], **6422**, 64220X, International Society for Optics and Photonics (2007).

[28] Huang, F., Ren, H., Wu, X., and Wang, P., "Flexible foveated imaging using a single risley-prism imaging system," *Opt. Express* **29**, 40072–40090 (Nov 2021).

[29] Li, A., Gao, X., Sun, W., Yi, W., Bian, Y., Liu, H., and Liu, L., "Inverse solutions for a risley prism scanner with iterative refinement by a forward solution," *Applied Optics* **54**(33), 9981–9989 (2015).

[30] Beltran-Gonzalez, A., Garcia-Torales, G., Strojnik, M., Flores, J., and Garcia-Luna, J., "Forward and inverse solutions for risley prism based on the denavit-hartenberg methodology," in [*Infrared Remote Sensing and Instrumentation XXV*], **10403**, 1040311, International Society for Optics and Photonics (2017).

[31] Duma, V.-F. and Dimb, A.-L., "Exact scan patterns of rotational risley prisms obtained with a graphical method: Multi-parameter analysis and design," *Applied Sciences* **11**(18) (2021).

[32] Wang, J., Ge, Y., and Chen, Z. D., "On the paraxial approximation and phase-gradient methods for risley prism inspired beam-steering metasurface antennas," in [*2021 Cross Strait Radio Science and Wireless Technology Conference (CSRSWTC)*], 336–338, IEEE (2021).

[33] Wen, Z., Ban, Y.-L., Yang, Y., and Wen, Q., "Risley-prism-based dual circularly polarized 2d beam scanning antenna with flat scanning gain," *IEEE Antennas and Wireless Propagation Letters* (2021).

[34] Li, Y., "Ruled surfaces generated by risley prism pointers: I. pointing accuracy evaluation and enhancement based on a structural analysis of the scan field inside the pointer," *JOSA A* **38**(12), 1884–1892 (2021).

[35] Yuan, L., Li, J., Huang, Y., Ma, R., Shi, J., Wang, Q., Wen, P., Ma, H., Li, M., and Wang, Z., "High-precision closed-loop tracking of moving targets based on rotational double prisms," *Optical Engineering* **60**(11), 114107 (2021).

[36] Montes-Flores, M., Garcia-Torales, G., and Strojnik, M., "A lab proof-of-concept of an extrasolar planet detection using a rotationally shearing interferometer," in [*Infrared Remote Sensing and Instrumentation XXIX*], **11830**, 118300O, International Society for Optics and Photonics (2021).

[37] Huang, F., Ren, H., Shen, Y., and Wang, P., "Error analysis and optimization for risley-prism imaging distortion correction," *Applied Optics* **60**(9), 2574–2582 (2021).

[38] Garcia-Torales, G., Strojnik, M., and Paez, G., "Risley prisms to control wave-front tilt and displacement in a vectorial shearing interferometer," *Applied Optics* **41**(7), 1380–1384 (2002).

[39] Gonzalez-Romero, R., Strojnik, M., and Garcia-Torales, G., "Theory of a rotationally shearing interferometer," *J. Opt. Soc. Am. A* **38**, 264–270 (Feb 2021).

[40] Bravo-Medina, B., Strojnik, M., and Kranjc, T., "Feasibility of planet detection in two-planet solar system with rotationally-shearing interferometer," in [*Infrared Remote Sensing and Instrumentation XXVII*], **11128**, 111280F, International Society for Optics and Photonics (2019).

[41] Strojnik, M. and Bravo-Medina, B., "Response of rotational shearing interferometer to a planetary system with two planets: simulation," in [*Modeling Aspects in Optical Metrology VII*], **11057**, 1105705, International Society for Optics and Photonics (2019).